Central European Journal of Energetic Materials, **2007**, *4*(1-2), 109-124.
ISSN 1733-7178

Quantitative Infra-Red Microscopy Method for the Determination of the Deterrent Diffusion Activation Energy in a Spherical Propellant

Laurence JEUNIEAU and Michel H. LEFEBVRE

Laboratory for Energetic Materials, Royal Military Academy
Av. de la Renaissance 30, 1000 Brussels, Belgium
E-mail: laurence.jeunieau@rma.ac.be

Pierre GUILLAUME

PB Clermont, S.A., Rue de Clermont 176, 4480 Engis, Belgium

Abstract: A calibration procedure for quantitative determination of dibutylphthalate concentration in a double base propellant is established. The best results are obtained by dividing an absorption band, characteristic of the dibutylphthalate, by an absorption band characteristic of the double base mixture. The influence of the nitroglycerin concentration on the linear calibration curve is investigated and it is shown that a linear relationship can be obtained for different concentrations of nitroglycerin by multiplying the absorbance ratio by the nitrocellulose concentration. The developed analysis protocol is applied to characterize quantitatively the deterrent concentration profile of a flattened ball propellant. Since the measured profile in a given propellant grain is dependent of the orientation of the analysed cross-section, geometrical and concentration factors are used to eventually describe the profile perpendicularly to the grain surface. The validated experimental procedure is then applied to study the characteristic of the diffusion process of the deterrent throughout the grain by artificial ageing at different temperatures. From these results, diffusion coefficients and diffusion activation energy of 154 ±15 kJ/mol have been obtained. Furthermore, a simulation program has been used to validate the used procedure for the calculation of the diffusion coefficient.

Keywords: infrared microscopy, deterrent diffusion, ageing

Introduction

Spherical propellants are used widely in small calibre weapons. They are easy to manufacture and their combustion properties can be tailored for different ammunition types by chemical modification of their surface composition. This surface modification usually consists of an impregnation by a deterrent which is only present along the surface and down to a certain depth and with a usually unknown and not fully controlled gradient. This deterrent concentration gradient results in a nearly constant pressure generation during the combustion process, compensating for the reducing burning surface area by a burning rate that increases with time.

The deterrent concentration profile has a great influence on the propellant combustion rate and the vivacity of the propellant. Therefore, the knowledge of the initial profile as well as its evolution during the lifetime of the propellant is of major importance and the migration rate of the deterrent into the propellant core during artificial ageing is a relevant factor for the determination of the shelf life of the propellant. This work establishes an experimental method for the determination of the deterrent profile inside the propellant grain and for the investigation of its diffusion process throughout the core of the grain. It is part of a large work program carried out by several nations to investigate the chemical and ballistic stability of ball powder [1-2]. The chemical stability of the propellant has also been investigated and results from this investigation have been presented by Wilker *et al.* [2].

Different methods of investigation have been used by many authors to measure the deterrent concentration profiles, for instance ^{14}C-radioisotope-labeled deterrents and autoradiographic [3-4] but these methods have the disadvantage that the propellant must be specially synthesised for this purpose. Staining and optical methods [5-6] have also been used but are not capable of directly measuring the concentration profiles and gradient. Infrared (IR) microscopy [7-11] and Raman microscopy [12-13] have been proved to be a powerful and efficient method for the determination of qualitative and quantitative concentration profiles of deterrents in propellants.

In this paper, IR microscopy has been used for the determination of the deterrent concentration profile in a ball powder double base propellant. We focussed on the influence of the nitroglycerin content on the calibration line in order to obtain a calibration valid for various types of double base propellants.

Using the developed calibration procedure, we determined the deterrent concentration in a flattened rolled ball propellants and the investigation on aged

propellants enables us to determine diffusion coefficients and diffusion activation energy.

Sample preparation and experimental set up

Reference samples

For the determination of the calibration line, double base propellants with a homogeneous content of (DBP) have been manufactured. Two types of propellants have been used, one with 11.0% of nitroglycerin and one with 26.0% of nitroglycerin. These propellants are mixed with increasing amounts of dibutylphthalate and with a solvent (tetrahydrofurane) to ease the manufacturing process. Mixing occurs at ambient temperature. This mixture has been extruded to obtain cylindrical propellant strands of about 2 mm in diameter. To increase homogeneity of the samples, extrusion is repeated twice. The extrusion chamber is at 80 °C. The manufactured samples are stored at 40 °C during a week to ensure complete evaporation of the tetrahydrofurane. The homogeneity of the sample is checked by IR microscopy. The nominal compositions of the reference samples are obtained by HPLC and are recorded in Table 1.

Table 1. Percentage of nitroglycerin (Ngl), dibutylphthalate (DBP) and nitrocellulose (NC) in the different manufactured samples

Type I	% Ngl	11.0	10.4	9.9	9.4	8.8
	% DBP	0.1	3.9	9.2	13.7	19.2
	% NC	88.9	85.7	80.9	76.9	72.0
Type II	% Ngl	26.6	25.3	24.0	22.6	21.3
	% DBP	0.0	4.7	8.7	14.4	18.8
	% NC	73.4	70.0	67.3	63.0	59.9

Aged samples

The propellant used for the investigation of the diffusion process is a double base propellant, containing 10.5% of nitroglycerin and on average 4.6% of DBP. It is a flattened propellant which can be geometrically modelled by an ellipsoid with a great axis of 660 μm and with two small axis of 360 μm. The propellant is aged at different temperatures. The ageing durations are given in Table 2.

Table 2. Ageing duration of the investigated propellants in days

T [°C] \ [d]	A	B	C	D	E	F	G	H
80	1.20	1.81	2.41	3.61	5.41	7.22	9.02	10.83
70	4.92	7.25	9.58	14.50	21.74	30.93	36.23	43.48
65	-	-	-	30.93	-	-	-	-
60	21.06	31.61	42.12	63.22	99	126.4	-	189
50	100.7	151.0	202	302	-	605	-	-

A, B, ...H are labels for different duration times.

Infrared microscopy

The propellant grains are embedded in a polyepoxy resin. 7 μm thick sections are prepared using a Leica microtome and a tungsten carbide knife.

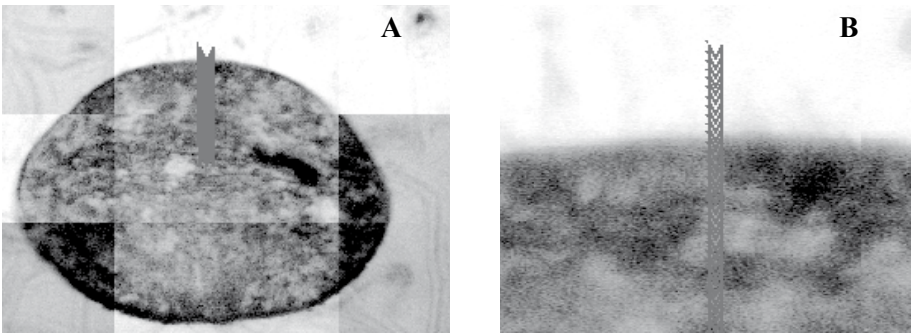

Figure 1. **A** Picture of a propellant cross section. **B** Enlargement of picture **A**, each label corresponds to a measurement position.

A Bruker Hyperion IR mounted on a Vector 33 Fourier-transform spectrometer is used in this study. A medium-band MCT (HgCdTe) detector in the microscope gives high sensitivity in the 4000-600 cm^{-1} range. Propellant grain cross section is placed on a KBr pellet and IR spectra are taken at 3 μm intervals. The Figure 1 shows a picture of a propellant section, each "M" mark represents a measurement position. A 15X cassegrain mirror objective is used to obtain the infrared spectra. The IR spectrometer is operated at a resolution of 4 cm^{-1} and 32 scans are acquired for each measurement position. The size of the aperture is 10 x 30 μm.

Results and Discussion

Calibration

As it is nearly impossible to obtain a propellant section of constant thickness, the calibration cannot be performed by using only the intensity of an absorption band characteristic of the DBP. To take into account the variation of the sample thickness, the absorption band characteristic of the DBP must be divided by an absorption band characteristic of the matrix (in this case mainly nitrocellulose).

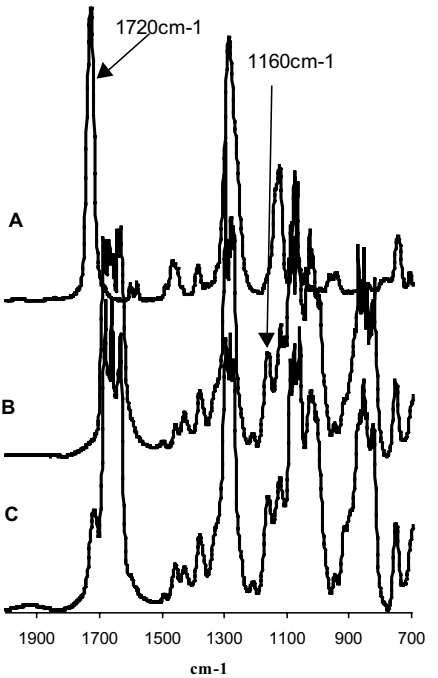

Figure 2. Infrared spectra of (A) pure DBP, (B) double base propellant (matrix), (C) DBP +matrix.

Figure 2 shows the IR spectra of the matrix of a double base propellant, DBP, and a mixture of both. In the literature, the C=O absorption band (1720 cm^{-1}) is always used for characterising the DBP. Different absorption band are used for characterising the nitrocellulose, either the absorption band at 2555 cm^{-1} [14], or 1160 cm^{-1} [15], or 1005 cm^{-1}. The ratios between the C=O absorption band and the above mentioned ones of NC have been tested extensively for the establishment of a linear calibration relationship.

The best calibration straight line is obtained by using the NC absorption band at 1160 cm^{-1}. To obtain a good calibration straight line, the analysed section must not be too thick; this condition can be converted into a condition on the absorbances. We have noticed that, for optimal analytical conditions, the absorbance of NC at 1160 cm^{-1} must range from 0.3 to 0.6 and that the absorbance of DBP at 1720 cm^{-1} must be lower than 1.6.

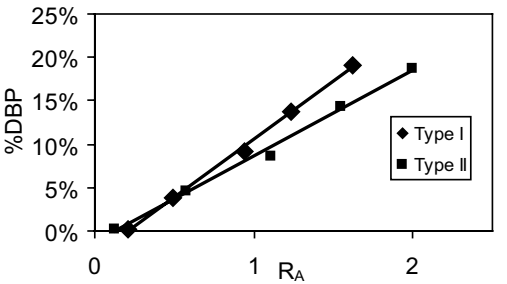

Figure 3. Calibration line obtained for the reference samples I and II. The abscissa R_A is defined in Eq. (1).

Table 3. Equation of the calibration linear regression for the two types of reference samples

	Linear regression	Correlation coefficient (r^2)
Type I	%DBP = 0.134 R_A – 0.013	0.995
Type II	%DBP = 0.099 R_A – 0.030	0.998

The calibration straight lines for the reference samples I and II (see Table 1) are shown in Figure 3. The equations of the two calibration straight lines are given in Table 3. The absorbance ratio used for the calibration is given by Eq. 1:

$$R_A = \frac{Max\ absorbance\ 1720\ cm^{-1}}{Max\ absorbance\ 1160\ cm^{-1}} \tag{1}$$

Influence of the nitroglycerin content

To establish the calibration regression line, the ratio between an absorption band characteristic of the DBP and with an absorption band characteristic of the nitrocellulose has been used. Therefore, the actual equation for the calibration should be:

$$\frac{[DBP]}{[NC]} = a\ R_A + b \tag{2}$$

where *a* and *b* are constant values and [DBP] and [NC] are concentration of dibutylphthalate and nitrocellulose respectively. As the variation of the nitrocellulose concentration in one propellant type (see Table 1) is not too important, a linear relationship is still obtained between the DBP concentration and the absorbance ratio (Figure 3).

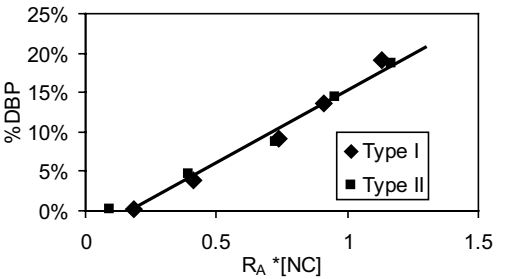

Figure 4. Percentage of DBP as a function of ratio of the NC and DBP absorption bands multiplied by the percentage of nitrocellulose. The label (Type I or II) refers to propellant with a different concentration in nitroglycerin (see Table 1).

But the range of nitrocellulose concentrations is different in the two types of reference sample, accounting for two different calibration lines. To be freed from this effect, the ratio between the two absorption bands has been multiplied by their respective nitrocellulose concentration. The obtained calibration line is shown in Figure 4 and the regression is:

$$[DBP] = 0.183\ R_A \times [NC] - 0.030 \quad (r^2 = 0.979) \tag{3}$$

It can be seen, that, by this procedure, a single useful calibration line can be obtained. The advantage of such a global calibration line is that it can be used for propellant with different nitrocellulose and nitroglycerin ratios and save the need of manufacturing specific reference samples for the characterisation of new composition propellants.

Deterrent concentration profile

A particularity of this work is that the investigated propellant is a flattened sphere of small size. It can be considered as a "torric disc" with an average thickness of 360 μm and an average diameter of 665 μm. Due to these geometrical characteristics, the position of the cut section in the sample is of great importance when one wants to obtain the concentration of the deterrent perpendicularly

to the grain surface. Ideally the section should pass by the centre of the particle, but practically it is not possible to be sure that the section passes trough the centre of the particle. Figure 5 shows schematically the influence of the cut section on the observed impregnation depth and Figure 6 shows the effect of this influence on a typical measured deterrent concentration profile. Note that profiles exhibiting discrepancies as shown in Figure 6 are not acceptable.

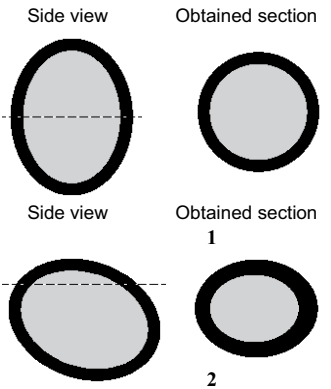

Figure 5. 1. Section in the centre of the particle. 2. Section above the centre of the particle. The dotted line corresponds to the position where the section is done. The dark zone represents schematically the portion of the grain impregnated with deterrent.

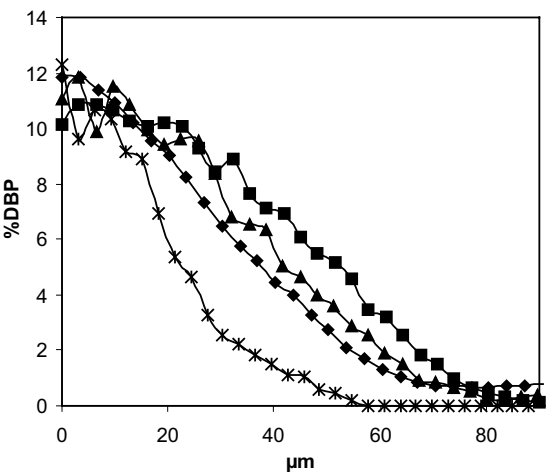

Figure 6. Typical deterrent concentration profiles for different sections of the same propellant particle. The origin of the abscissa is the surface of the propellant grain.

Consequently, a specific post-processing procedure should be adjusted upon to analyse properly and consistently the results from the IR analyses. The decision criteria to validate the measurements and to consider a recorded concentration profile as "representative" and "relevant" are the following:

- The recorded deterrent concentration profile is integrated over the entire cross section to obtain the average deterrent concentration. As the nominal average concentration is known by HPLC measurements these two values are compared and profiles with integrated values close to the nominal values are retained.
- The actual deterrent penetration depth must be the smallest observed since, if the section does not pass through the centre of the particle, the observed penetration depth will be always greater than the actual one (see Figure 5).

We noticed that the smallest observed deterrent penetration depth corresponds usually with a good value of the average deterrent concentration, and this good correlation between the two criteria backs up their relevance.

Quantification of the molecular diffusion

Samples of the deterred double base propellants have been aged according to the timetable in Table 2. The evolution of the deterrent concentration profile is then studied using the above-described analytical procedure. Figure 7 shows the obtained DBP concentration gradients for ageing at 80 °C. Each profiles is the result of averaging at least three individual profiles.

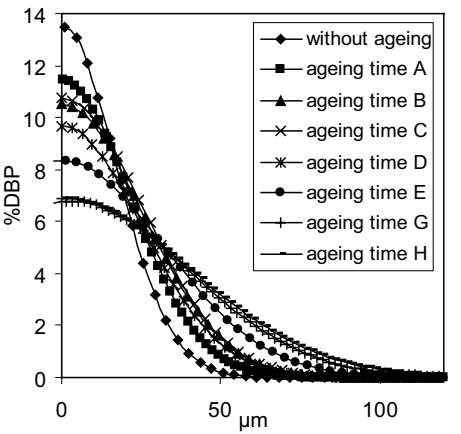

Figure 7. Concentration profile of DBP in the propellant for different ageing durations at 80 °C.

From these records, the diffusion coefficient (D) can be calculated [16-17]. The Fick's diffusion model is used to fit the concentration profiles. The equation for a one-dimensional diffusion in anisotropic media may be expressed by:

$$\frac{\partial c}{\partial t} = D \frac{\partial^2 c}{\partial x^2} \tag{4}$$

where c is the diffusant concentration (kg/m^3), t the diffusion time (s), D the diffusion coefficient (m^2/s) and x the Cartesian space coordinate (m).

Providing constant diffusion coefficient within the segment where diffusion takes place, general solutions of Eq. (4) can be obtained for a variety of initial and boundary conditions. Equation (5) describes the concentration profile as function of time and space, when initiated by an instantaneous planar source:

$$c(x,t) = \frac{s}{\sqrt{\pi D t}} e^{\frac{-x^2}{4Dt}} \tag{5}$$

where s is the surface concentration of diffusant (kg/m^2).

By using the deterrent concentration at the particle surface, Eq. (5) can be rewritten as

$$c(x,t) = c(x,t) e^{\frac{-x^2}{4Dt}} \tag{6}$$

In this equation, the entire deterrent is supposed to be at the surface of the propellant at the initial time ($t = 0$). In our work, a deterrent concentration profile is already present before the ageing of the propellant. By consequence, the time in Eq. (6) is not equal to the time of ageing but to the summation of the time needed to obtain the initial deterrent concentration profile observed before ageing (t_1) and to the ageing time (t_i).

The experimental curves (Figure 7) are numerically fitted to obtain the value of $c(0,t)$ and of the corresponding parameter Dt. The diffusion coefficient can then be calculated using the set of Eq. (7):

$$\begin{cases} Dt_1 & \text{from initial profile, before ageing} \\ Dt_i & \text{from analysed profiles, after ageing time} \\ t_i\text{-}t_1 & \text{ageing duration} \end{cases} \tag{7}$$

Figure 8 shows the different values of the diffusion coefficient obtained

for the different times of ageing at 80 °C and gives an idea of the precision of the FTIR technique. It can be observed that a rather constant value is obtained.

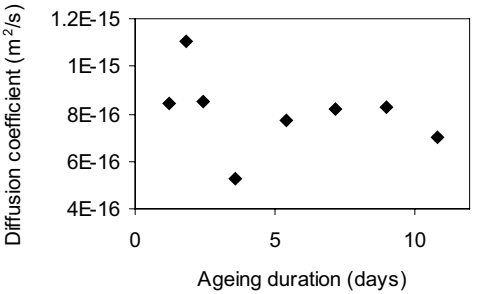

Figure 8. Values of the diffusion coefficient obtained for the different ageing times at 80 °C.

The different average diffusion coefficients obtained for the different ageing temperature are in Table 4.

Table 4. Average values of the diffusion coefficient obtained for the different ageing temperatures

Temperature (°C)	Diffusion coefficient (m^2/s)
80	$8.1\ 10^{-16}$
70	$2.0\ 10^{-16}$
65	$9.0\ 10^{-17}$
60	$4.1\ 10^{-17}$
50	$4.1\ 10^{-18}$

Calculation of the activation energy of the diffusion process

From the diffusion coefficients obtained at different temperatures, the diffusion activation energy can be calculated using an Arrhenius law (Eq. 8)

$$D = D_0 \exp^{(-E_D/RT)} \tag{8}$$

Figure 9 shows the linear regression done for the calculation of the diffusion activation energy. From this linear regression a diffusion activation energy of 154 ±15 kJ/mol has been calculated.

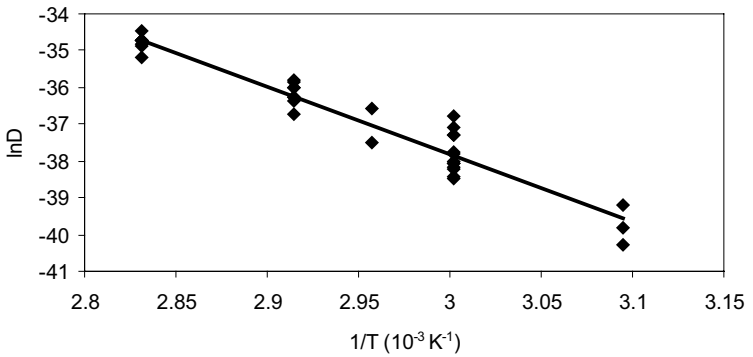

Figure 9. Arrhenius plot of the diffusion coefficient.

Validation of the diffusion coefficient calculation

The procedure used for the determination of the diffusion coefficient is based on the Fick's diffusion law for a planar geometry. In our case, the diffusion geometry is closer to a spherical geometry than to a planar geometry. The Fick's diffusion law for a planar geometry is given by Eq. (4) and the Fick's diffusion law for a spherical geometry is given by Eq. (9) where r is the radius of the spherical particle [18-19].

$$\frac{\partial C}{\partial t} = D\left(\frac{\partial^2 C}{\partial r^2} + \frac{2}{r}\frac{\partial C}{\partial r}\right) \tag{9}$$

To validate the calculated diffusion coefficient, the deterrent diffusion has been simulated in a planar geometry and in a spherical geometry. Using a forward time centred space differentiating scheme, Eq.(4) can be rewritten as [19-20]:

$$\frac{C_j^{n+1} - C_j^n}{\Delta t} = D\left[\frac{C_{j+1}^n - 2C_j^n + C_{j-1}^n}{\Delta x^2}\right] \tag{10}$$

where C_j^n is the deterrent concentration with j corresponding to the spatial subscript and n corresponding to the time subscript, Δt is the time step used for the calculation and Δx is the spatial step for the definition of the initial concentration profile. In the numerical calculation, the following stability criterion must be taken into account (using von Neumann stability analysis method):

$$\frac{2D\Delta t}{\Delta x^2} \leq 1 \tag{11}$$

The boundary condition given by the following equation has been used.

$$C_1^{n+1} = D\left[\frac{C_2^n - C_1^n}{\Delta x^2}\right]\Delta t + C_1^n \tag{12}$$

In a spherical geometry, Eq. (9) can be calculated by the discrete equation:

$$C_j^{n+1} = D\left[\frac{C_{j+1}^n - 2C_j^n + C_{j-1}^n}{\Delta r^2} + \frac{2}{r}\frac{C_{j+1}^n - C_j^n}{\Delta r}\right]\Delta t + C_j^n \tag{13}$$

The deterrent concentration profiles that should have been obtained after propellant ageing have been simulated for a spherical and planar geometry. These calculations have been performed using the diffusion coefficient resulting from the linear regression used for the determination of the activation energy. Figure 10 shows the simulated and experimental values for propellant K80A and K80G. For propellant K80A, there is no difference between the calculated values using a planar or a spherical geometry. For propellant K80G, there is a slight difference between the calculated values using a planar or spherical geometry. The observed difference for propellant K80G is due to the higher ageing time.

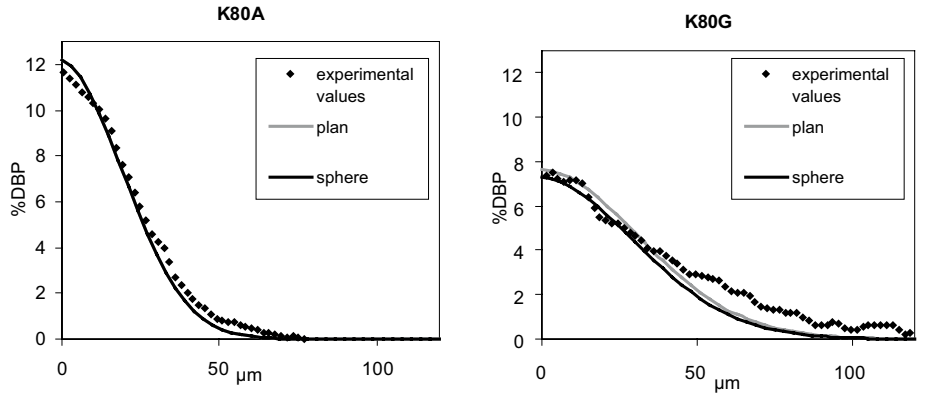

Figure 10. Deterrent concentration profiles obtained by calculation using a spherical and plan geometry for propellant K80A and K80G. The experimental values are also indicated.

The difference between the simulated values and the experimental values is due to the experimental uncertainty on the diffusion coefficient. The observed differences between experimental values and simulated values are greater than

the difference between the simulated values obtained with a planar or spherical geometry. By consequence, the using of the planar geometry as none influence on the calculation of the activation energy, at least for the ageing time and for the propellant geometry used in this work.

Conclusions

An analytical method for quantitative determination of dibuthyphthalate in a flattened rolled ball propellant has been established. It has been shown that the calibration line for the DBP concentration determination depends on the nitroglycerin concentration. A single calibration line may be used if the concentration value is multiplied by the nitrocellulose concentration. This calibration procedure has the great advantage that it can be used for all double base propellants and therefore specific reference samples must not be manufactured.

The developed protocol has been used for the determination of deterrent concentration profiles in a flattened rolled ball propellant. The deterrent penetration depth depends on the analysed cross section but the use of an appropriate post-processing procedure enables us to describe this profile unambiguously.

This method has permitted to characterise the deterrent diffusion during ageing and a diffusion activation energy of 154 ±15 kJ/mol has been obtained.

The deterrent concentration profiles have been recalculated using a planar and spherical geometry. It has been observed that there is none or a slight difference between the simulated results obtained using a planar or a spherical geometry. A good correlation has been obtained between the experimental and the simulated results. These simulation procedure permits to obtain the deterrent concentration profiles for other ageing times and other ageing temperatures than the one that have been used for the determination for the activation energy.

This work has been a start on a large program on the chemical and physical stabilities of ball propellants. This program involves comparison between the evolution of the ballistic properties during ageing and the deterrent diffusion process, comparison between the decomposition activation energy and the diffusion activation energy.

Acknowledgement

Some authors (L.J. and M.H.L.) acknowledge financial support from the Belgian Ministry of Defense through a grant for scientific research ACOS-Strat-STER&T-AR01.

References

[1] Jeunieau L., Lefebvre M.H., Guillaume P., Wilker S., Heeb G., Frank S., Chevalier S., Stability Analyses of Rolled Ball Propellants. Part II- Ballistic Stability, *35th Int. Ann. Conf. ICT*, Karlsruhe, June 29-July 2, **2004**.

[2] Wilker S., Guillaume P., Lefebvre M. H., Chevalier S., Jeunieau L., Pantel G., Ticmanis U., Stottmeister L., Stability Analyses of Rolled Ball Propellants Part 1: Microcalorimetric Studies and Stabilizer Depletion, *34th Int. Ann. Conf. ICT*, Karlsruhe, 24-27 June **2003**.

[3] Brodman B.W., Devine M.P., Finch R.W., MacClaren M.S., Autoradiographic Determination of the di-n -Butyl-Phthalate Concentration Profile in a Nitrocellulose Matrix, *J. Appl. Polym. Sci*., **1974**, *18*, 3739.

[4] Brodman B.W., Devine M.P., Chemical Interactions and Their Effect on the Small Arms Propellant Deterring Process, *J. Ballistics*, **1978**, *2*, 51.

[5] Fong C.W., Cooke C., Diffusion of Deterrents into a Nitrocellulose-Based Small Arms Propellants. The Effect of Deterrent Structure and Solvent, *J. Appl. Polym. Sci.,* **1982**, *27*, 2827.

[6] Stiefel L., Devine M.P., Depth of Penetration of Deterrent in Representative U.S. Small Arms Propellants, **1979**, *3*, 515.

[7] Rat M., Lacroix G., A New Method to Determine Migration Profiles of Low Molecular Weight Constituants in Propellants: FTIR Microscopy Equiped with a Motorized Stage, *25th Int. Ann. Conf. ICT,* Karlsruhe, June 28-July 1, **1994**.

[8] Pesce-Rodriguez R. A., Miser C. S., McNesley K. L., Fifer R. A., Kessel R. A., Strauss B.S., Characterization of Solid Propellant and its Connection to Aging Phenomena, *Appl. Spectrosc.*, **1992**, *46*, 1143.

[9] Vogelsanger B., Ossala B., Brönnimann E., The Diffusion of Deterrents and Blasting Oils into Propellants Observed by FTIR Microspectroscopy, *10th Symposium on chemical problems connected with the stability of explosives*, **1996**, 305.

[10] Louden J. D., Kelly J., Infrared Mapping of Deterrents (Morderents) in Nitrocellulose Based Propellant by Fourier-Transform Infrared Microscopy, *Anal. Appl. Spectrosc.,* **1991**, *2*, 90.

[11] Varriano-Marston E., An Infrared Microspectroscopy Method for Determining Deterrent Penetration in Nitrocellulose-Based Propellant Grains, *J. Appl. Polym. Sci.*, **1987**, *33*, 107.

[12] Louden J. D., Kelly J., Phillipson J., Methylcentralite Concentration Profiles in Monoperforated Extruded Nitrocellulose and Nitrocellulose/Nitroglycerine Propellant Grains by Raman Microspectroscopy*, ibid.*, **1989**, *37*, 3237.

[13] Louden J. D., Kelly J., Phillipson J., Raman Microspectroscopic Determination of the Methyl Centralite (*N,N'*-Dimethyl-*N,N'*-Diphenylurea) Concentration Profile in a Nitrocellulose Extruded Mono-Perforated Small Arms Propellant, *J. Raman Spectrosc.*, **1985**, *18*, 137.

[14] Louden J. D., Duncan I. A., Kelly J., Speirs R. M., The Application of Infrared Microimaging for the Determination of the Distribution, Penetration Depth, and Diffusion Profile of Methyl Centralite and Dibutylphthalate Deterrents in Nitrocellulose Monoperforated Propellant, *J. Appl. Polym. Sci.*, **1993**, *49*, 275.
[15] Vogelsanger B., Ossala B., Brönnimann E., The Diffusion of Deterrents into Propellants Observed by FTIR Microspectroscopy- Quantification of the Diffusion Process, *Propellants, Explos., Pyrotech.,* **1996**, *21*, 330.
[16] Ossala B., Vogelsanger B., Brönnimann E., FTIR-Spektroskopie – eine vielseitige Methode zur Analytik von Nitrocelulose und Treibladingspulvern, *25th Int. Ann. Conf. ICT,* Karlsruhe, Germany, 28 June- 1 July, **1994**.
[17] Atkins P. W., Physical Chemistry, Third Edition, Oxford University Press, **1996**.
[18] Crank J., The Mathematics of Diffusion, Oxford Science Publications, **1975**.
[19] Boddington T., Luo R., Halford-Maru P., Aspects of Convolution-Deconvolution Voltemmetry, http://WWW.logosem.com/condecor/pdf/APPONOTE9.pdf
[20] Numerical recipes in C: The Art of Scientific Computing, Cambridge University Press, **1988**.